







Doc.no: SW\_TEST\_MC3\_VALi2\_\_00000000T000000\_99999999T999999\_0101  
 Rev: 1A  
 Date: September 11, 2012

# Swarm Level 2 Processing System

British Geological Survey (BGS)  
 National Space Institute - DTU Space (DTU)  
 Delft Institute of Earth Observation and Space Systems (DEOS)  
 Helmholtz Centre Potsdam - German Research Centre for Geosciences (GFZ)  
 Eidgenössische Technische Hochschule Zürich (ETH)  
 Institut de Physique du Globe de Paris (IPGP)  
 with additional contributions from  
 NASA Goddard Space Flight Center (GSFC)  
 University of Colorado (CIRES)  
 Charles University Prague (CUP)

## Intermediate validation of Swarm Level 2 Products

SW\_TEST\_MIN\_3DMi2a\_00000000T000000\_99999999T999999\_0101  
 SW\_TEST\_MIN\_3DMi2a\_00000000T000000\_99999999T999999\_0101  
 SW\_TEST\_MCR\_3DMi2\_\_00000000T000000\_99999999T999999\_0101

<b>Prepared:</b>	Alexei Kuvshinov	<b>Prepared:</b>	Christoph Pütke
Function:	Team leader 	Function:	Team member 
Date:	September 11, 2012	Date:	September 11, 2012
<b>Prepared:</b>	Jakub Velínský 	<b>Approved:</b>	Alexei Kuvshinov
Function:	Team member	Function:	Team leader 
Date:	September 11, 2012	Date:	September 11, 2012



---

## Record of changes

<b>Reason</b>	<b>Description</b>	<b>Rev.</b>	<b>Date</b>
Initial version	Release for AR2	1A	September 11, 2012



# Contents

1	Introduction . . . . .	4
1.1	Purpose . . . . .	4
1.2	Scope . . . . .	4
1.3	Executive Summary . . . . .	4
2	Applicable and Reference Documentation . . . . .	4
2.1	Reference Documents . . . . .	4
2.2	Abbreviations . . . . .	5
3	Validation of Swarm Level 2 products . . . . .	5
3.1	Objective . . . . .	5
3.2	Validation Process for the Mantle Induction Products . . . . .	5
3.3	Role of Scientist in the Loop . . . . .	6
4	Intermediate Validation Report . . . . .	6
4.1	Input products and data . . . . .	6
4.2	Output Products . . . . .	6
4.3	Validation Results . . . . .	7
4.4	Criteria . . . . .	16
5	Conclusions . . . . .	17

# 1 Introduction

## 1.1 Purpose

The purpose of this document is to describe and illustrate the processes and tests applied to the intermediate validation of the MIN\_3DMi2a, MIN\_3DMi2b and MCR\_3DMi2\_ products generated in the V2 test. The detailed product names under inspection are:

SW\_TEST\_MIN\_3DMi2a\_00000000T000000\_99999999T999999\_0101,  
SW\_TEST\_MIN\_3DMi2b\_00000000T000000\_99999999T999999\_0101,  
SW\_TEST\_MCR\_3DMi2\_00000000T000000\_99999999T999999\_0101.

For the purpose of the V1 and V2 tests, the products use a simulated dataset covering the period from 1998/07/01 00:45 to 2002/12/31 23:15. The products are valid at any time (time-independent). The version number 0101 refers to the products generated in V2 testing (version number 0001 was used for V1 tests).

## 1.2 Scope

The document applies to the development phase and to the implementation and operational phases of the project.

## 1.3 Executive Summary

The Swarm products

SW\_TEST\_MIN\_3DMi2a\_00000000T000000\_99999999T999999\_0101,  
SW\_TEST\_MIN\_3DMi2b\_00000000T000000\_99999999T999999\_0101,  
SW\_TEST\_MCR\_3DMi2\_00000000T000000\_99999999T999999\_0101,

have undergone a series of validations and checks by partner ETH/CUP. The ETH/CUP SILs opinion is that the products are validated and therefore suitable for release as the intermediate products.

# 2 Applicable and Reference Documentation

## 2.1 Reference Documents

The following documents contain supporting and background information to be taken into account during the activities specified within this document.

[RD-1 ] Swarm Level 1b Product Definition, SW-RS-DSC-SY-0007

[RD-2 ] Product Specification for L2 Products and Auxiliary Products, SW-DS-DTU-GS-0001

[RD-3 ] Earth Explorer File Format Standards Doc. No: PE-TN-ESA-GS-0001 ESA ESTEC, Noordwijk, The Netherlands

[RD-4 ] Swarm Level 2 Product Data Handbook, SW-HB-DTU-GS-0001

[RD-5 ] Swarm Level 2 Processing System, ETH Sub-System Acceptance Test Report V2, SW-TR-ETH-GS-0004\_SS\_ATR\_V2.

## 2.2 Abbreviations

Acronym	Description
CAT-1	Category 1 products
CUP	Charles University in Prague
ESA	European Space Agency
ETH	Eidgenössische Technische Hochschule Zürich
FD	Frequency domain
L2PS	Level 2 Processing Segment
SIL	Scientist in the Loop
PDGS	Payload Data Ground Segment
TD	Time domain
V1	Version 1
V2	Version 2
VAL	Validation
1-D	One-dimensional
3-D	Three-dimensional

Table 1: List of abbreviations.

## 3 Validation of Swarm Level 2 products

### 3.1 Objective

The objective of this document is to verify and validate the Level 2 CAT-1 intermediate product output. The next stage of verification is carried out using auxiliary data from independent sources to confirm that the output is scientifically valid and feasible. The purpose is

- (a) to ensure that no obvious mistakes or errors have been made in the production of the Level 2 output, and
- (b) to give non-expert users confidence that the product released have been thoroughly inspected.

### 3.2 Validation Process for the Mantle Induction Products

Mantle induction products are difficult to compute for a number of reasons, principally the lack of suitable data and the long periods required. The `MIN_3DMi2_` and `MCR_3DMi2_` are novel products for the Swarm mission. They represent a 3-D average mantle conductivity model of the Earth obtained by the FD and TD methods, and the 2-D maps of induction  $C$ -responses at discrete frequencies, respectively.

The following steps are undertaken to validate, then promote the product for release to the ESA Payload Data Ground Segment (PDGS):

- (a) Intermediate L2 products `MIN_3DMi2a`, `MIN_3DMi2b`, `MCR_3DMi2_` are produced by the Level 2 Processing Segment (L2PS) processing chain.
- (b) An internal validation of the products is produced in the form of intermediate product validation reports `MI3_VALi2_` and `MC3_VALi2_`. As only a combined validation of all products is scientifically meaningful, both reports have the same content.

The intermediate products including their internal validation are distributed via PDGS to the L2PS. The British Geological Survey performs an independent validation of the products and produces a report, which will include the internal validation.

### 3.3 Role of Scientist in the Loop

The validation of the products is actively undertaken by the scientists in the loop (SIL) at ETH/CUP. The SILs check that the products conform to scientific expectations using a series of tests and also check that the products are correctly formatted for release. The SILs produce a validation report and release the products back to the ESA PDGS for further independent validation. The role of the SILs is to ensure that the outputs meet the criteria of being valid scientific products.

## 4 Intermediate Validation Report

The mantle conductivity models are 3-D models of the conductivity in the Earth. Besides the dominant dependence on depth, they also provide information about lateral variations of conductivity, i.e., its dependence on latitude and longitude. Lateral variations of electrical conductivity in the Earth are, in general, poorly known, meaning that an independent validation of the mantle conductivity and induction products is limited.

In the production phase, the main task of validation will be to provide cross-comparison of the products of the TD and FD approaches and to compare the products to the previously published 1-D model AUX\_MCM based on CHAMP/Ørsted/SAC-C satellite data and to the 1-D model recovered in the production phase.

For the purpose of V1 and V2 testing, simulated data in the TDS-1 dataset were prepared using a known, artificial target conductivity model. Therefore, the 3-D conductivity products MIN\_3DMi2a and MIN\_3DMi2b can be compared directly against this model. Naturally, this will not be possible for models based on actual satellite data.

### 4.1 Input products and data

The following products are used in the assessment of the MIN\_3DMi2a, MIN\_3DMi2b, and MCR\_3DMi2\_:

Product	Type	Comment
SW_TEST_AUX_MCM_2_00000000T000000_99999999T999999_0002.DBL	Mantle conductivity model	Independent 1-D model from CHAMP satellite data
SW_TEST_MIN_1DMi2_00000000T000000_99999999T999999_0101.DBL	Mantle conductivity model	1-D conductivity model from the 1-D chain
SW_TEST_MCR_1DMi2_00000000T000000_99999999T999999_0101.DBL	C-responses	Global 1-D C-responses from the 1-D chain
target.DBL	Mantle conductivity model	Known 3-D target conductivity model (V1, V2 tests only)

Table 2: Input products used for validation

### 4.2 Output Products

The output products from this validation report are:

Swarm Level 2 Magnetic field Products:

SW\_TEST\_MIN\_3DMi2a\_00000000T000000\_99999999T999999\_0101,

SW\_TEST\_MIN\_3DMi2b\_00000000T000000\_99999999T999999\_0101,

SW\_TEST\_MCR\_3DMi2\_00000000T000000\_99999999T999999\_0101,

Swarm Level 2 Validation Products:

SW\_TEST\_MC3\_VALi2\_00000000T000000\_99999999T999999\_0101.

### 4.3 Validation Results

The tests were conducted between 2012/08/31 and 2012/09/12.

#### Frequency domain approach

For the FD approach, the data are Fourier transformed, and a set of coefficients (of the spherical harmonic expansion of the magnetospheric field) at 20 logarithmically spaced periods between 2 days and 64 days are selected for analysis.

The conductivity of five inhomogeneous layers with thicknesses of 200 km each at depths between 10 km and 1000 km is sought. The known conductance of the surface layer representing crust and oceans (surface conductance map) is scaled to a thickness of 10 km and fixed. The 1-D conductivity below 1000 km is fixed as well. This signifies that target model and recovered model necessarily have a different stratification.

Forward computations are performed on a regular grid with resolution of  $5^\circ \times 5^\circ$ . For inversion, each layer of the domain is parameterized with spherical harmonics up to degree and order 5, resulting in  $5 \times (5 \times (5 + 2) + 1) = 180$  model parameters.

In order to compare target model and recovered models quantitatively, the overlapping sections must be regarded individually. An analysis is depicted in Figure 1. In the top 400 km (first and second row), where conductivity is quasi-constant, errors are in general very small, but a ghost effect of the underlying large-scale anomaly is visible. The three small-scale anomalies are not recovered. This was expected, as such small-scale structures can not show up in spherical harmonic data of degree 5 and less.

Errors are larger between 400 km and 600 km (third row). Conductivity of both background and large-scale anomaly are recovered well, errors are marked at the boundary between anomaly and background. The shape of the anomaly is very blurred, the recovery is especially poor in the South Pacific. Errors however do not exceed one order of magnitude anywhere.

The largest errors are seen in the overlap region between 600 km and 700 km (fourth row). While the anomaly is recovered well, the low conductivity of the background is overestimated by about one order of magnitude. This is due to the non-coincidence of stratification in this depth region and the general difficulty in recovering resistive regions.

Figure 2b presents the recovered conductivity in the depth range of the anomaly in the target model, i.e. 400–700 km, as a weighted average of the 3rd and 4th layer recovered in the inversion,  $\sigma_{400-700 \text{ km}} = \frac{2}{3}\sigma_{400-600 \text{ km}} + \frac{1}{3}\sigma_{600-800 \text{ km}}$ . By combining information from both layers, the full anomaly is recovered, including the South Pacific.

Errors are reduced to less than half an order of magnitude between 700 km and 800 km (fifth row), partially compensating for the overestimation of conductivity between 600 km and 700 km (note that these two “layers” actually represent one layer). Errors are very low between 800 km and 1000 km.

The solution is regularized by downweighting of higher harmonics in the lateral direction and

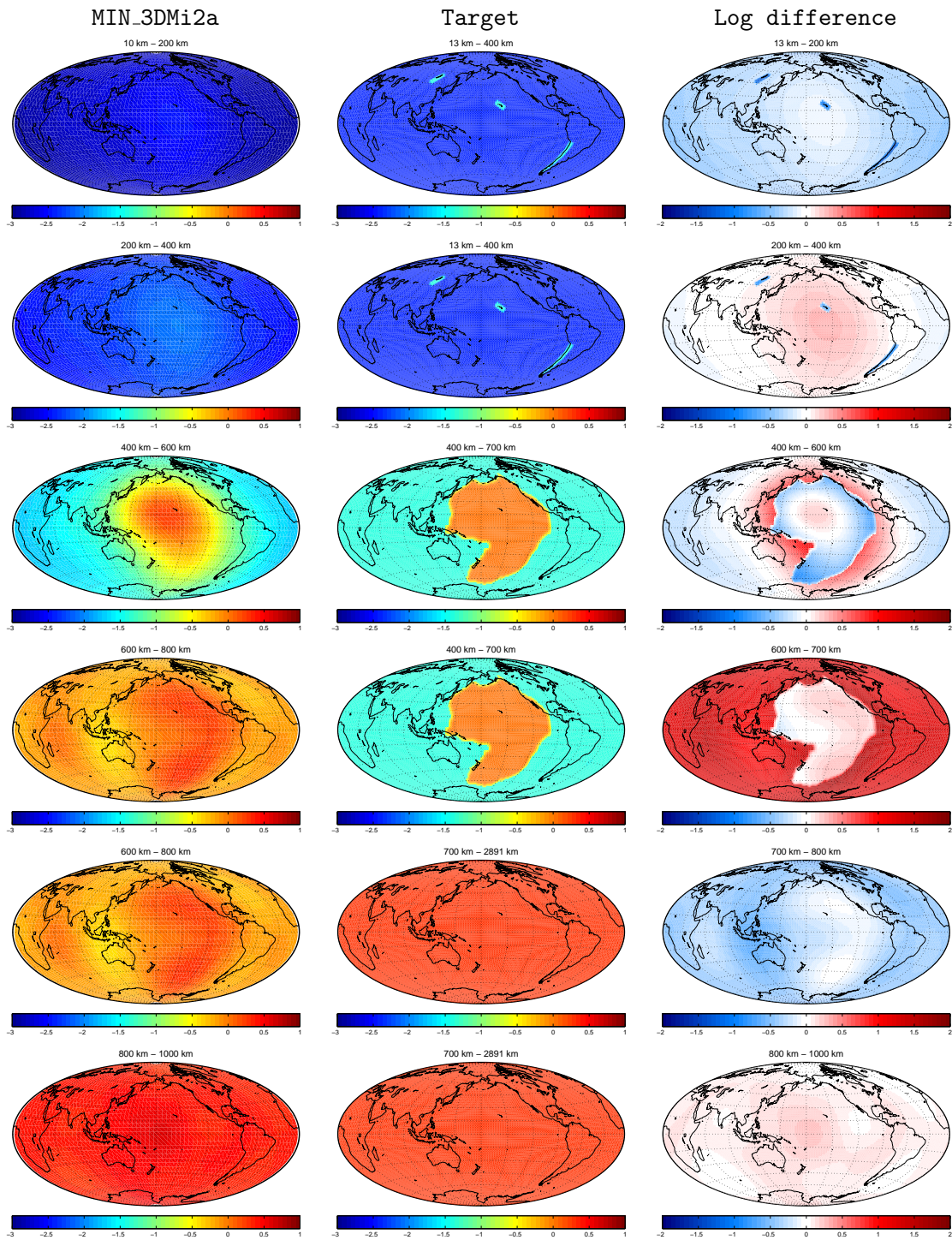


Figure 1: Comparison of the MIN\_3DMi2a model (left column) with the known target model (middle column). The right column shows the decadic logarithm of the ratio (or equivalently, the difference of logarithms) between the recovered and target conductivity. The radial interval is marked in each plot.



by a finite difference approximation of the gradient in the vertical direction. Inversion is started with strong regularization, the result of the 1-D inversion MIN\_1DMi2\_ is used as starting model. After reaching convergence, the amount of regularization is reduced and a new inversion run is started. The result for the previous regularization parameter is used as starting model.

Fig. 2a summarizes the performed runs in term of their final data misfit and regularization term. L-curve analysis generally suggests to choose the solution in the knee of the trade-off curve. As the data of the V2 test contain errors, we decided to pick a stronger regularized solution. The results shown in Figure 1 have been obtained for a regularization parameter of 20. A visual inspection of the inversion results for all regularization parameters confirmed this choice.

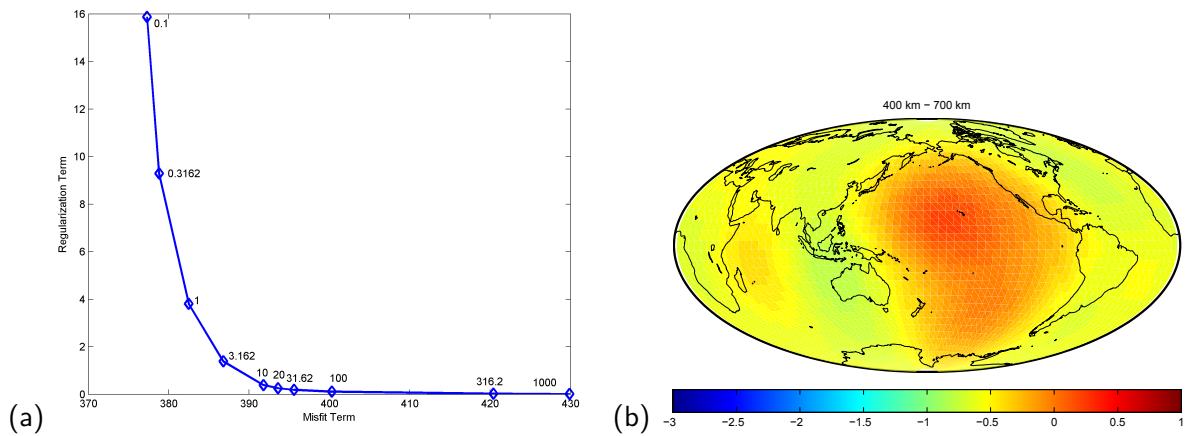


Figure 2: (a) Trade-off curve (so-called L-curve) for the frequency-domain approach. The results depicted in Figure 1 correspond to a regularization parameter of  $\lambda = 20$ . (b) Recovered conductivity in the range 400–700 km, obtained by weighted averaging of the results shown in Figure 1.

### Time-domain approach

In the TD chain, the conductivity model is parameterized in a similar way to the FD chain. Logarithm of resistivity is expanded into spherical harmonic functions up to degree and order of 5 in 5 layers 200 km thick. Surface conductance map AUX\_OCM\_, rescaled to uniform thickness of 13 km, is placed on the top of the model. The forward solution is truncated at degree and order 8, and uses 88 radial nodes, corresponding to parallelization of the solver on 22 CPU cores. The entire 4.5 years time series of MMA\_SHAi2C\_ is used.

The LMQN iterations were parallelized in two runs with decreasing regularization parameter  $\lambda$  in a leapfrog manner: the first run used values of  $10^{-0}$ ,  $10^{-2}$ ,  $10^{-4}$ , the second run values of  $10^{-1}$ ,  $10^{-3}$ ,  $10^{-5}$ . Preliminary analysis of the L-curve suggested optimal value of  $\lambda$  between  $10^{-2}$  and  $10^{-1}$ . A third run was therefore performed for values of  $5 \times 10^{-2}$  and  $2 \times 10^{-2}$ . The L-curve is shown in the left part of Figure 3. In the right part of the figure, we show the convergence of the LMQN iterations arranged by decreasing  $\lambda$ . Value of  $\lambda = 2 \times 10^{-2}$  is closest to the maximum inflection point of the L-curve, and model with this regularization was selected as MIN\_3DM\_2b candidate.

Figure 4 compares the MIN\_3DMi2b against the TDS-1 synthetic model (target.DBL). Note

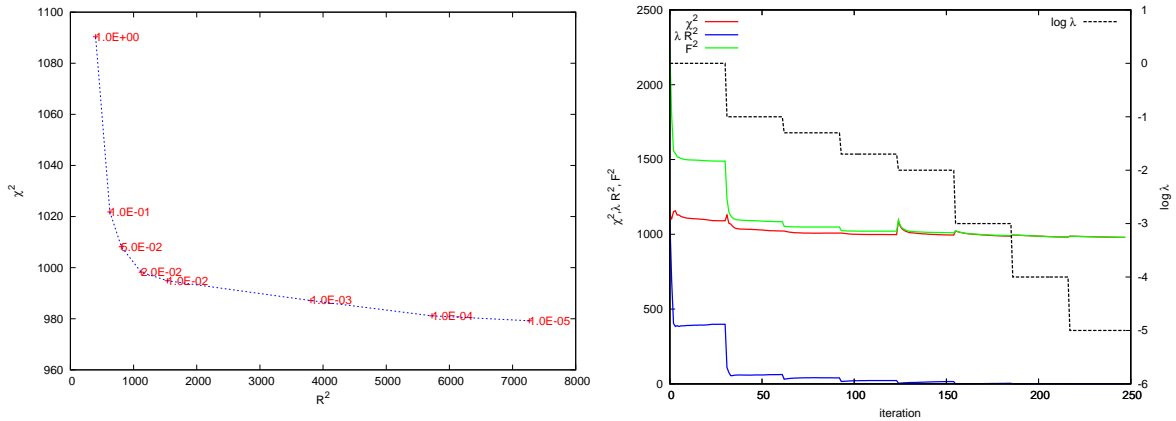


Figure 3: Left: The L-curve showing tradeoff between data misfit  $\chi^2$  and regularization  $R^2$  for different choices of regularization parameter  $\lambda$ . Right: Convergence of the LMQN minimization sorted by decreasing  $\lambda$ . Note that  $F^2 = \chi^2 + \lambda R^2$  is the total penalty function.

that the two models use different structure of layers, partially overlapping. The electrical conductivity of the target heterogeneity placed at 400 km depth, as well as of the background conductivity at this depth is recovered within 1 order of magnitude. Discrepancies occur due to the choice of layer boundaries, the target model in fact lies outside of the model space explored by the inversion. For example, the layer 5571.2–5771.2 in the MIN\_3DMi2b model partially recovers the heterogeneity in the 5671.2–5971.2 layer of the target model, and partially the conductivity of the homogeneous lower mantle below it (3480.0–5671.2). That stresses the importance of parameterization choice in the inversion of actual satellite data — the position of layer boundaries should comply with well known positions of phase transitions in the Earth’s mantle.

In the uppermost part of the model (above 400 km depth), the results of the inversion overshoot the target model significantly. Using a series of alternative runs, it has been shown that this discrepancy can be explained by the presence of large conductivity jump, more than 2 orders of magnitude, at the depth of 400 km in the synthetic target model. By fixing the conductivity above 400 km close to the correct value, e.g. as recovered by 1-D inversion chain MIN\_1DMi2-, conductivity in the target zone is then underestimated, as the regularization prevents large jump across the interface. Using less regularized model allows for correct reconstruction of the 1-D background, but leads to lateral oscillations. Anisotropic regularization would probably solve the problem, but that would be a solution tailored specifically to the target model, not much relevant to the realistic, smoother conductivity increase across the transition zone.

On the other hand, the 1-D lower mantle conductivity (below 700 km) is well recovered from the data.

### Comparison of MIN\_3DMi2a and MIN\_3DMi2b products

Both 3-D conductivity products are compared directly in Figures 6 and 5. In Figure 6, laterally averaged, radially dependent conductivity profiles are shown for both models as well as for the target model. In addition, the span of lateral variations in each layer is marked by dashed lines. Detailed cross sections are then summarized and compared in Figure 5. Both products are able to recover the target model within the required specifications. The differences between them can be assigned to slightly different implementation of regularization, and its balancing against the

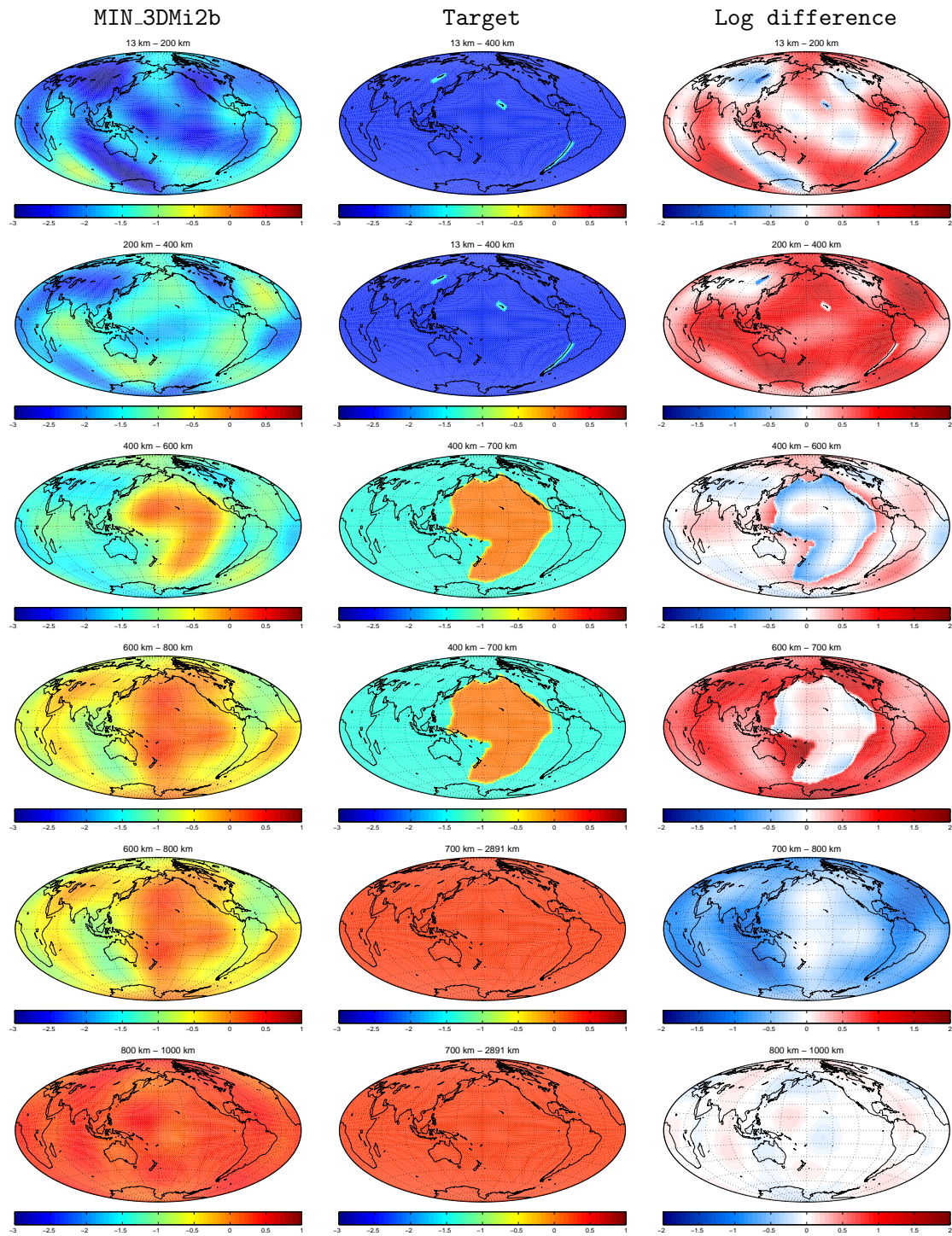


Figure 4: Comparison of the MIN\_3DMi2b model (left column) with the known target model (middle column). The right column shows the decadic logarithm of ratio (or equivalently, the difference of logarithms) between the recovered and target conductivity. The radial interval is marked in each plot.

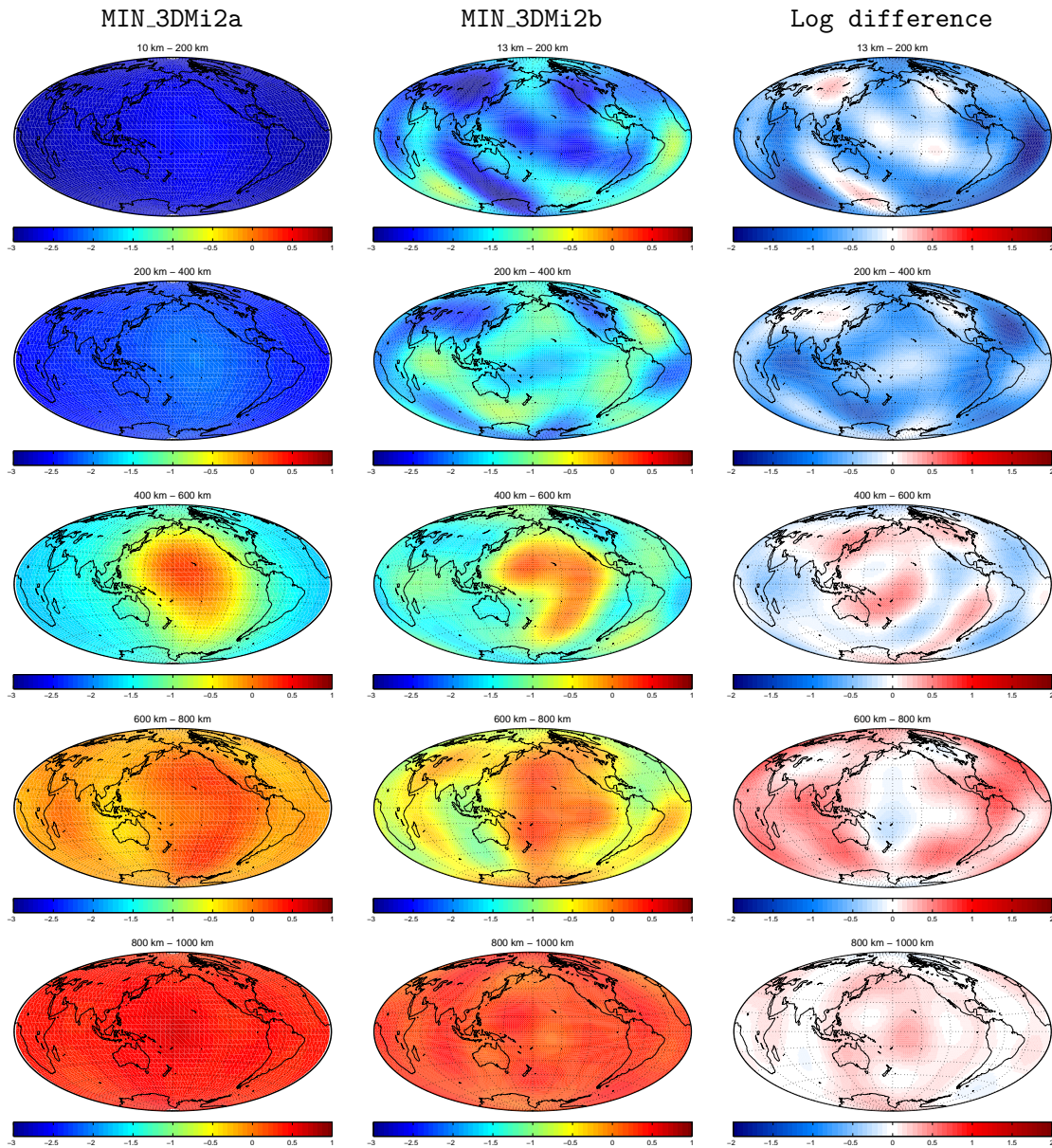


Figure 5: Comparison of the MIN\_3DM.2a (left column) and MIN\_3DM.2b model (middle column). The right column shows the decadic logarithm of ratio (or equivalently, the difference of logarithms) between the recovered and target conductivity. The radial interval is marked in each plot.

data misfit. The MIN\_3DMi2a product is closer to the target model in the upper mantle, where the MIN\_3DMi2b product overestimates the conductivity and contains some spurious lateral variations. On the other hand, the MIN\_3DMi2b product offers more accurate recovery of the shape of the main heterogeneity in the 400–600 km depth range.

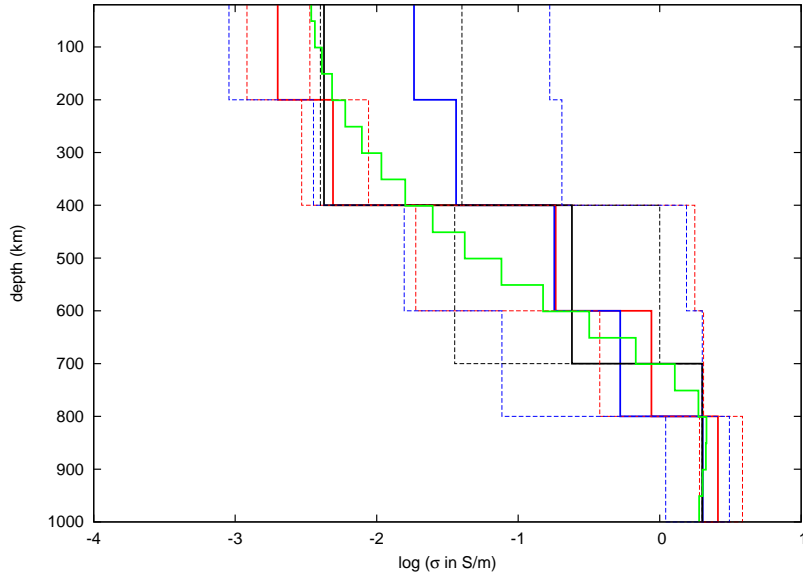


Figure 6: Comparison of the radial conductivity profiles as recovered by the MIN\_3DMi2a model (red) and the MIN\_3DMi2b model (blue) with the known target model (black). Solid lines show the average conductivity as function of depth, dashed lines correspond to minimum and maximum conductivity at given depth for each model. In addition, the 1-D product MIN\_1DMi2\_ is shown in green.

### Validation of $C$ -responses maps

Global maps of  $C$ -responses were computed with the horizontal spatial gradient method, i.e.

$$C(\mathbf{r}, \omega) = -\frac{B_r(\mathbf{r}, \omega)}{\nabla_{\perp} \cdot \mathbf{B}_T(\mathbf{r}, \omega)}, \quad (1)$$

where the magnetic field and its angular divergence were synthesized from the experimental spherical harmonic coefficients. The responses were calculated on a regular mesh of  $10^{\circ} \times 10^{\circ}$  for 28 logarithmically spaced periods between 12 hours (Nyquist period) and 200 days.

Maps of real and imaginary part of the  $C$ -responses for selected frequencies as well as maps of the respective coherencies are plotted in Figure 7. The surface conductance map only shows up in the imaginary part of the responses. While there is no trace of the small-scale anomalies in the depth range 10–400 km, the large-scale pacific plate anomaly is present for periods from 1.5 days to about 100 days and mainly visible in the real part. Note that coherencies are generally low in the equatorial region due to the disappearance of the radial component, cf. Eq. (1). The results in this region are therefore not trustworthy. Coherencies in mid-latitudes are generally good for periods above 2 days and get better with increasing period.

In a 1-D model, the  $C$ -response is easily computed directly from the conductivity structure. In particular, its real part is a measure of the penetration depth  $\delta$  for electromagnetic waves in a conductor. Figure 8 compares maps of the 3-D  $C$ -responses with maps of 1-D  $C$ -responses computed directly for each grid point from the local 1-D conductivity structure of the target model for two selected frequencies. The general agreement between the figures is good, taking into account the low coherencies of the  $C$ -responses in the equatorial region and the fact that small-scale structures can not be resolved with the applicable data. Also note that the direct computation from conductivity does not take into account 3-D effects, thus the results close to

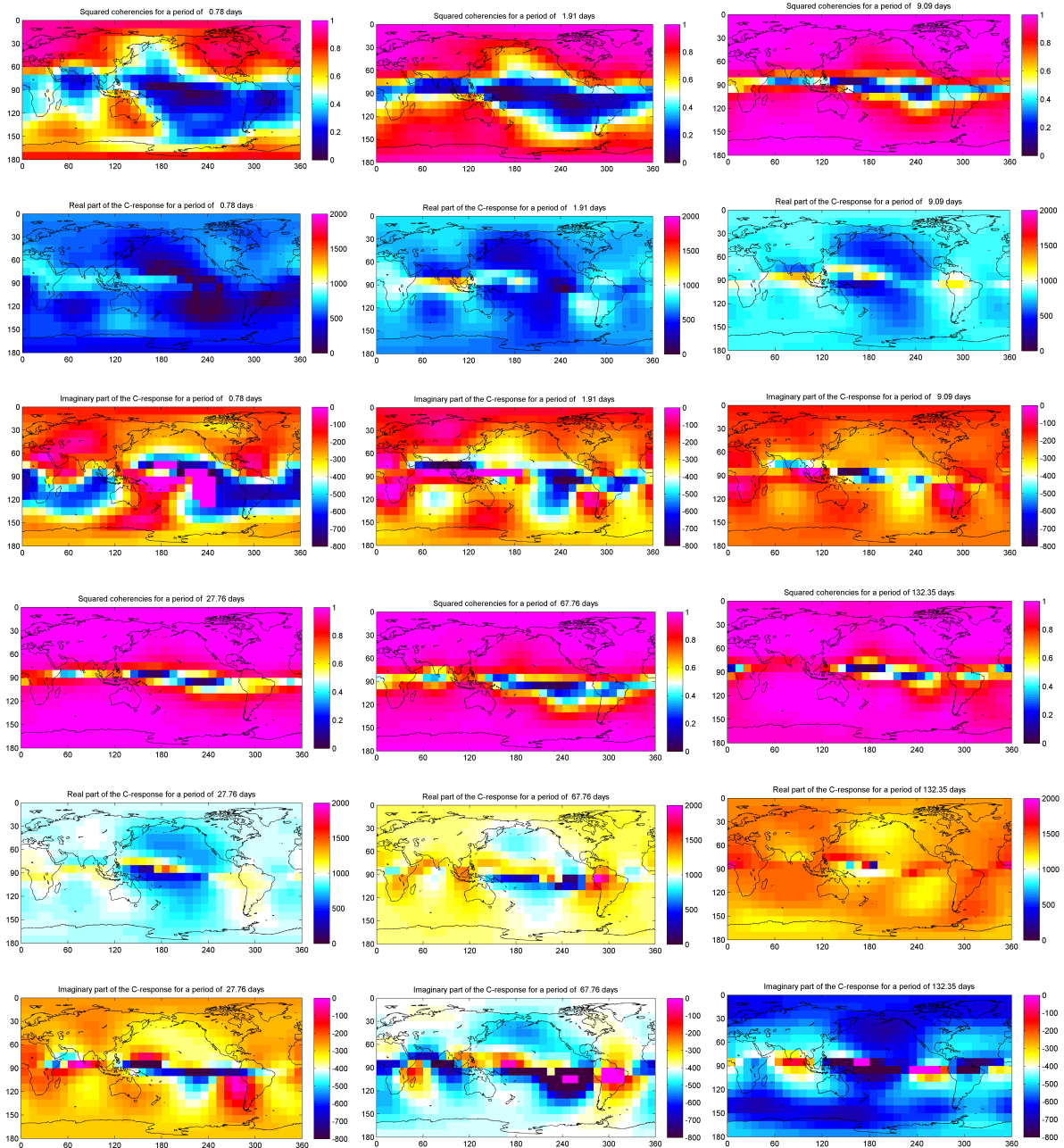


Figure 7: World maps of recovered  $C$ -responses for periods of 0.8 days, 1.9 days, 9.1 days, 27.8 days, 67.8 days and 132.35 days (from top left to bottom right). Each panel shows squared coherencies (no unit), real and imaginary part (both in km).

conductivity jumps are not trustworthy.

Figure 9 finally shows a comparison between the global 1-D  $C$ -responses obtained in the 1-D inversion of the  $P_1^0$ -coefficient (product MCR\_1DMi2\_) and the 3-D  $C$ -responses of product MCR\_3DMi2\_. For this purpose, the 3-D responses of all grid points (excluding the equatorial region between  $\pm 27^\circ$ ) are plotted in the same grid. As expected, they cluster around the 1-D responses, thereby providing a further validation of the product.

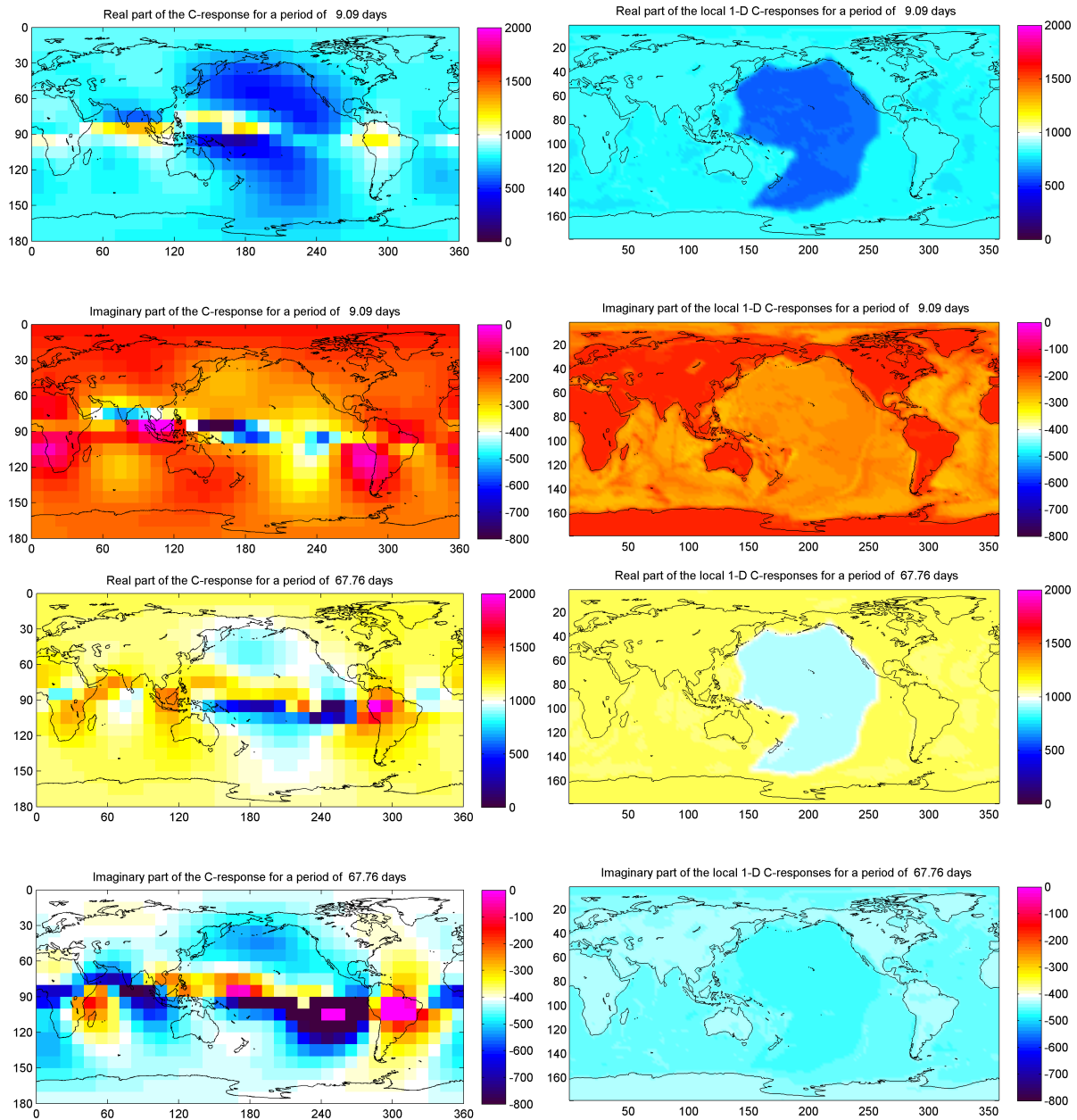


Figure 8: Comparison between real and imaginary parts of 3-D  $C$ -responses (left) and 1-D  $C$ -responses (using the local 1-D conductivity structure, right) for periods of 9.1 days (top) and 67.8 days (bottom). Units are kilometres.

### Format compatibility

The products

SW\_TEST\_MIN\_3DMi2a\_00000000T000000\_99999999T999999\_0101,

SW\_TEST\_MIN\_3DMi2b\_00000000T000000\_99999999T999999\_0101

have been successfully written and subsequently read using the subroutines from the MantleConductivityI0.f90 module.

The product

SW\_TEST\_MCR\_3DMi2\_00000000T000000\_99999999T999999\_0101

has been successfully written and subsequently read using the subroutines from the `CResponsesIO.f90` module (see `SwarmL2/smarth-eth/eth-internal/I0_subroutines` in the `svn`) as documented in [RD-5].

Conformance to the format was also checked visually against specifications (in particular: header comments, number and indexing of layers/periods, lateral grid dimensions.)

#### 4.4 Criteria

The following criteria are suggested to cross-check the validity of the products.

Product	Test	Criteria	Pass
MIN_3DMi2a	comparison with TDS-1 target model	difference within 1 order of magnitude	Yes (V1, V2 only)
MIN_3DMi2a	Read using <code>MantleConductivityIO</code>	Successfully read	Yes (see [RD-5])
MIN_3DMi2a	comparison with 1-D model <code>AUX_MCM_</code>	difference of averaged profile within 1 order of magnitude	N/A for V1, V2 tests
MIN_3DMi2a	comparison with 1-D model <code>MIN_1DMi2_</code>	difference of averaged profile within 1 order of magnitude	Yes
MIN_3DMi2b	comparison with TDS-1 target model	difference within 1 order of magnitude	Yes (V1, V2 only)
MIN_3DMi2b	Read using <code>MantleConductivityIO</code>	Successfully read	Yes (see [RD-5])
MIN_3DMi2b	comparison with 1-D model <code>AUX_MCM_</code>	difference of averaged profile within 1 order of magnitude	N/A for V1, V2 tests
MIN_3DMi2b	comparison with 1-D model <code>MIN_1DMi2_</code>	difference of averaged profile within 1 order of magnitude	Yes
MIN_3DMi2a MIN_3DMi2b	cross-comparison	difference within 1 order of magnitude	Yes
MCR_3DMi2_	comparison with 1-D <i>C</i> -responses computed from TDS-1 target model	difference < 500 km	Yes (V1, V2 only)
MCR_3DMi2_	Read using <code>CResponsesIO</code>	Successfully read	Yes (see [RD-5])
MCR_3DMi2_	comparison with 1-D <i>C</i> -responses	difference < 500 km	Yes

Table 3: Validation criteria



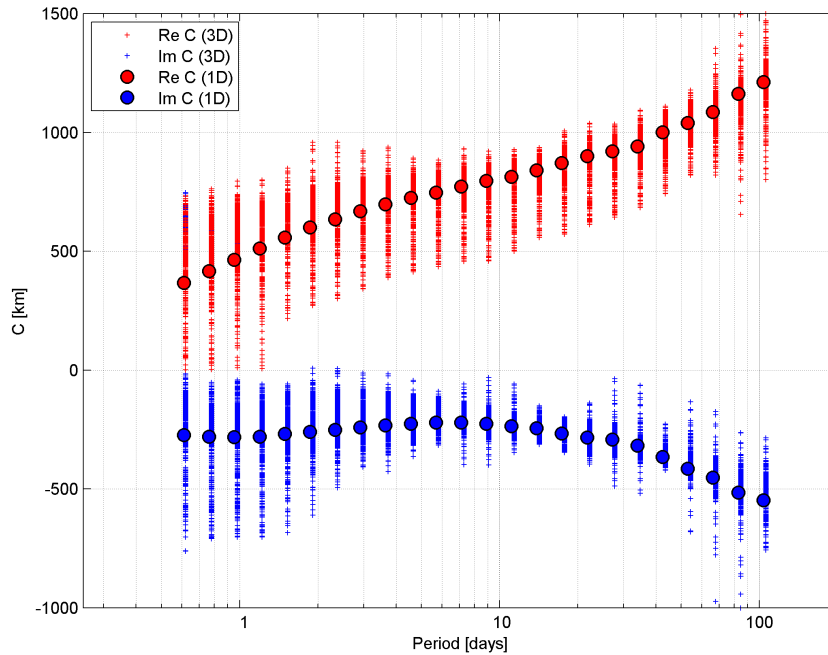


Figure 9: Comparison between 1-D  $C$ -responses (product MCR\_1DMi2\_) and 3-D  $C$ -responses (product MCR\_3DMi2\_) at latitudes higher than  $\pm 27^\circ$ .

## 5 Conclusions

The Swarm products

SW\_TEST\_MIN\_3DMi2a\_00000000T000000\_99999999T999999\_0101,

SW\_TEST\_MIN\_3DMi2b\_00000000T000000\_99999999T999999\_0101,

SW\_TEST\_MCR\_3DMi2\_00000000T000000\_99999999T999999\_0101,

have undergone a series of validations and checks by partner ETH/CUP. In particular:

- (a) They have been found to conform to the format specification.
- (b) They have recovered the TDS-1 target conductivity model within 1 order of magnitude accuracy.

The ETH/CUP SILs opinion is that the products are validated and therefore suitable for release as the intermediate product.